Regular Article

MYELOID NEOPLASIA

JAK2V617F$^+$ myeloproliferative neoplasm clones evoke paracrine DNA damage to adjacent normal cells through secretion of lipocalin-2

Yuki Kagoya,[1] Akihide Yoshimi,[1] Takako Tsuruta-Kishino,[1] Shunya Arai,[1] Takashi Satoh,[2,3] Shizuo Akira,[2,3] and Mineo Kurokawa[1]

[1]Department of Hematology and Oncology, Graduate School of Medicine, The University of Tokyo, Tokyo, Japan; and [2]Laboratory of Host Defense, World Premier International Research Center Initiative, Immunology Frontier Research Center, and [3]Department of Host Defense, Research Institute for Microbial Diseases, Osaka University, Osaka, Japan

Key Points

- JAK2V617F$^+$ MPN clones induce paracrine DNA damage into coexisting normal clones through secretion of lipocalin-2.

- Lipocalin-2 suppresses normal hematopoiesis via p53 pathway activation and gives relative growth advantage to MPN clones.

Genetic instability is strongly involved in cancer development and progression, and elucidating the mechanism could lead to novel therapeutics for preventing carcinogenesis. Philadelphia-negative myeloproliferative neoplasms (MPNs) are clonal myeloid disorders with a high prevalence of JAK2V617F mutation, and transformation to acute myeloid leukemia through accumulation of additional mutations is a major complication in MPNs. Here, we showed that JAK2V617F$^+$ cells conferred paracrine DNA damage to neighboring normal cells as well as to themselves through increased reactive oxygen species (ROS). We screened candidate factors responsible for the effect and found that lipocalin-2 (Lcn2) is overexpressed in JAK2V617F$^+$ cells and that short hairpin RNA–mediated knockdown of Lcn2 significantly alleviated the paracrine DNA damage. Normal hematopoietic cells showed elevated ROS levels through increased intracellular iron levels when treated with lipocalin-2, which led to p53 pathway activation, increased apoptosis, and decreased cellular proliferation. In contrast, JAK2V617F$^+$ cells did not suffer from lipocalin-2–induced growth suppression resulting from attenuated p53 pathway activation, which conferred a relative growth advantage to JAK2V617F$^+$ clones. In summary, we demonstrated that JAK2V617F-harboring cells cause paracrine DNA damage accumulation through secretion of lipocalin-2, which gives proliferative advantage to themselves and an increased risk for leukemic transformation to both JAK2V617F$^+$ and JAK2V617F$^-$ clones. (Blood. 2014;124(19):2996-3006)

Introduction

Myeloproliferative neoplasms (MPNs) constitute a group of diseases associated with increased production of mature myeloerythroid cells and/or platelets. Besides chronic myeloid leukemia, which is driven by the BCR-ABL fusion gene, the three most prevalent diseases in MPNs are polycythemia vera, essential thrombocythemia, and primary myelofibrosis. An acquired somatic mutation in the tyrosine kinase JAK2 gene resulting in a valine-to-phenylalanine substitution at position 617 (JAK2V617F) is most commonly seen in patients with BCR-ABL$^-$ MPN, which leads to constitutive activation of JAK-STAT pathway.[1-5] One of the most dismal complications in MPNs is their transformation to acute myeloid leukemia (AML), which is seen in 4% to 8% of patients with polycythemia vera or essential thrombocythemia within 20 years and in 8% to 23% of primary myelofibrosis patients in the first 10 years.[6-10] Although the JAK2V617F mutation is critically involved in the pathogenesis of MPNs, as verified in different murine MPN models, the mutation alone cannot induce leukemia in those models.[11-18] Recent studies have identified that acquisition of several gene alterations, including ASXL1, RUNX1, TET2, DNMT3A, IDH1/2, and TP53, is associated with leukemic transformations.[19-25] However, the fundamental mechanism involved in the increased risk for accumulation of genetic aberrations in MPNs remains to be elucidated. In addition to genotoxic agents used for treatment of MPNs,[26,27] some MPN-intrinsic factors should contribute to leukemic transformation, considering that the event also occurs in treatment-naïve patients.[8]

Curiously, the AML cells transformed from JAK2V617F$^+$ MPNs frequently lack the JAK2 mutation: 3 of 4, 9 of 17, and 9 of 16 patients developed JAK2 wild-type (WT) leukemia after JAK2-mutant MPNs in previous studies.[28-30] These results strongly indicate that the leukemia cells are derived from JAK2V617F$^-$ clones co-existing with JAK2V617F$^+$ clones in MPN phase. Although one of the driving factors might be the JAK2V617F-mediated genetic instability associated with the hyper-recombination phenotype,[31] it cannot explain the emergence of JAK2V617F$^-$ leukemia. In this study, we investigated the pathogenesis underlying the risk for leukemic transformation from MPNs by using a mouse model induced by transplantation of JAK2V617F-transduced bone marrow cells; we found that JAK2V617F$^-$ clones within MPN bone marrow also accumulate DNA damage and could have increased risk for progressing to leukemia.

There is an Inside Blood Commentary on this article in this issue.

The publication costs of this article were defrayed in part by page charge payment. Therefore, and solely to indicate this fact, this article is hereby marked "advertisement" in accordance with 18 USC section 1734.

Methods

Mice

In murine experiments, 8- to 10-week-old female C57BL/6 mice purchased from Japan SLC, Inc. (Shizuoka, Japan) were used. *Trp53*-knockout mice on a C57BL/6 background were obtained from RIKEN BRC (Tsukuba, Japan; Acc. No. CDB0001K).[32] *Lcn2* knockout mice on a mixed 129/sv-C57BL/6 background were established as previously described.[33] WT littermates were used as controls. All animal experiments were approved by the University of Tokyo Ethics Committee for Animal Experiments.

Reagents and antibodies

JAK2 inhibitor ruxolitinib (INCB018424) was purchased from Adooq Bioscience (Irvine, CA) and used at 100 nM for in vitro analysis. For in vivo studies, mice were treated with the inhibitor at an oral dose of 125 mg/kg. *N*-acetyl-*L*-cysteine, deferoxamine mesylate, and nutlin-3 were from Sigma-Aldrich, and recombinant mouse and human lipocalin-2 were from R&D Systems. In the apoptosis assay, cells were stained with Annexin V-APC (BD Biosciences) and analyzed by flow cytometry. Intracellular reactive oxygen species (ROS) production was measured with the 2′,7′-dichlorodihydrofluorescein diacetate fluorescent dye (Life Technologies). Cells were incubated with 35 μM 2′,7′-dichlorodihydrofluorescein diacetate for 30 minutes at 37°C. Antibodies used for experiments are summarized in supplemental Table 1 available at the *Blood* Web site.

Retrovirus production and bone marrow transplantation assays

Plat-E packaging cells were transiently transfected with each retrovirus vector, and the supernatants were used for infection. The MPN mouse model was established by transducing pGCDNsam-JAK2V617F-internal ribosome entry site (IRES)-enhanced green fluorescent protein (EGFP) into c-Kit⁺ bone marrow cells and injecting the green fluorescent protein (GFP)–positive cells into lethally irradiated (9.5 Gy) mice. Murine hematopoietic cell line 32D cells were transduced with pGCDNsam-JAK2V617F-IRES-EGFP, pGCDNsam-WT-JAK2-IRES-EGFP, or the empty EGFP vector and hemagglutinin-tagged pMYs-neo-murine Mpl.[34] For analyzing ROS levels, Kusabira-Orange–containing plasmids instead of EGFP were transduced.

Flow cytometry

Each fraction from normal or MPN bone marrow was isolated by using a FACSAria II cell sorter (Becton Dickinson). Analysis was performed with FlowJo software (Treestar, Ashland, OR).

Immunofluorescence analysis

Immunofluorescence staining of cells was performed as previously described.[35] Briefly, cells were fixed with 3.7% formaldehyde in phosphate-buffered saline, permeabilized by treatment with 0.2% Triton-X, and blocked with 1% bovine serum albumin in phosphate-buffered saline. The slides were incubated with primary antibodies at 4°C, followed by incubation with Alexa Fluor 488 goat anti-mouse immunoglobulin G (IgG; Life Technologies) and TO-PRO3 (Molecular Probes). Because the transplanted bone marrow cells expressed GFP, Alexa Fluor 647 goat anti-mouse IgG (Life Technologies) and 4,6 diamidino-2-phenylindole were used for analysis. Fluorescence images were captured with an Olympus FluoView FV10i confocal microscope. The mean intensity of intranuclear 8-hydroxy-2-deoxyguanosine was measured within a region of interest placed within the nucleus by using the Fluoview software. The background-subtracted fluorescence intensity was calculated in each cell, and the average intensity with standard deviation was calculated.

Immunoblotting

In each experiment, total-cell lysates were subjected to immunoblotting. Membranes were probed with the primary antibodies followed by horseradish peroxidase–labeled anti-mouse or anti-rabbit IgG antibodies (Santa Cruz

Biotechnology). Detection was performed with Immunostar LD western blotting detection reagent (Wako) and an LAS-3000 image analyzer (FujiFilm).

Analysis of microarray data

We analyzed publicly available gene expression microarray data, including murine and human samples with accession numbers GSE21842 and GSE9827. A set of CEL files were downloaded from Gene Expression Omnibus and normalized by using the justRMA function from the affy package of Bioconductor. For screening of genes with elevated expression in JAK2V617F⁺ cells compared with their normal counterparts, the expression values of individual genes were compared between groups by using the RankProd analysis, and the significantly elevated genes, as determined by false discovery rate <0.05 in both expression data, were selected.

Quantitative real-time PCR

Quantitative real-time polymerase chain reaction (PCR) was carried out on the LightCycler480 system (Roche) by using SYBR Green reagents according to the manufacturer's instructions. The results were normalized to *Gapdh* levels. Relative expression levels were calculated by using the 2-ΔΔCT method.[36] The primer sequences are summarized in supplemental Table 2.

shRNA interference

Gene-specific short hairpin RNAs (shRNAs) were designed and cloned into pSIREN-RetroQ-ZsGreen vectors (supplemental Table 2). Control shRNA is a nonfunctional construct provided from Clontech. JAK2V617F⁺ 32D cells were transduced with each vector and purified by flow cytometry by using an fluorescein isothiocyanate filter on the basis of the difference in fluorescence intensity.

Measurement of lipocalin-2 levels

To obtain cell conditioned media (CM), 32D cells were cultured for 24 hours at a concentration of 1×10^6 cells per milliliter in RPMI medium with 10% fetal bovine serum and 10% WEHI-3B supernatant. Human bone marrow mononuclear cells were cultured in RPMI medium supplemented with 10% fetal bovine serum, 25 ng/mL of stem cell factor, and 10 ng/mL of interleukin-3 (IL-3), IL-6, and FMS-like tyrosine kinase-3. The culture supernatants were collected after 48 hours. The concentration of lipocalin-2 was measured with murine or human Lipocalin-2 ELISA Kit (R&D Systems) based on a 4-parameter logistic regression model generated from the standard dilution curve in each assay.

Luciferase assay

32D-JAK2V617F cells were transiently transfected with pGL4.14[luc2/Hygro] with WT or mutant *Lcn2* promoter fragments provided by Dr. M.R. Green.[37] The cells were harvested 48 hours after transfection and assayed for luciferase activity in duplicate with a dual luciferase kit (Piccagene; TOYO B-Net) according to the manufacturer's protocol.

### Measurement of intracellular iron levels

Intracellular iron concentration was measured by using an iron assay kit according to the manufacturer's instructions (Metallo assay; AKJ Global Technology). Total-cell lysates collected from 32D cells were used for measurements after the addition of 1M hydrochloric acid at a final concentration of 0.05 M. Intracellular iron concentration was corrected with the total amount of protein and described as picograms per microgram of protein.

Statistical analysis

Statistical significance of differences between different groups was assessed with a 2-tailed unpaired or paired Student *t* test. Differences were considered statistically significant at a *P* value of less than .05.

Study approval

Patient-derived bone marrow cells and serum were obtained from the Department of Hematology and Oncology, The University of Tokyo
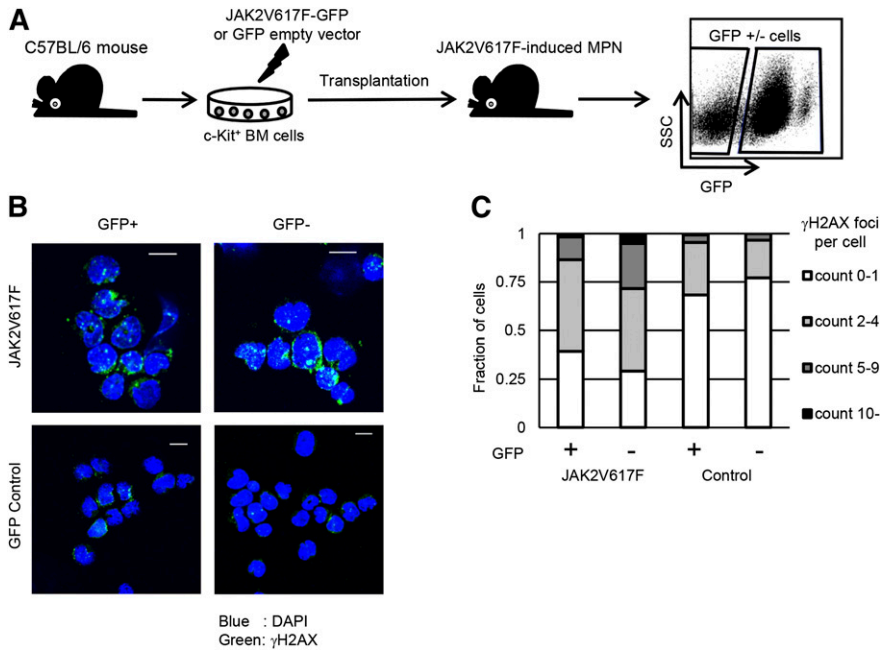
Figure 1. JAK2V617F-harboring bone marrow cells induce DNA damage response in neighboring normal cells in a paracrine manner. (A) Schematic representation of the following experiments. Murine bone marrow c-Kit^{+} cells were retrovirally transduced with JAK2V617F-IRES-GFP or control GFP and transplanted into sublethally irradiated mice. The reconstituted bone marrow cells were sorted on the basis of GFP positivity. SSC, side scatter. (B) Representative immunofluorescence images for γH2AX foci formation (Alexa Fluor 647: green) in GFP^{+/−}Lin[−]c-Kit^{+} cells in the MPN or control bone marrows. Nuclei were stained with 4,6 diamidino-2-phenylindole (DAPI) (blue). (C) Average distribution of the numbers of γH2AX foci per nucleus is shown. More than 100 cells were counted in individual specimens. Experiments were performed for 3 mice in each model. Scale bars: 10 μm.

Hospital, Tokyo, Japan. The study was approved by the ethical committee of the University of Tokyo, and written informed consent was obtained from all patients whose samples were collected in accordance with the Declaration of Helsinki.

Results

Normal hematopoietic cells within JAK2V617F-induced MPNs are susceptible to DNA damage

To examine the accumulation of DNA damage in the bone marrow cells of JAK2V617F-induced MPNs, we analyzed a murine model of JAK2V617F[+] MPNs (Figure 1A). MPN bone marrow cells contained both GFP[+] and GFP[−] fractions, and we confirmed that JAK2 phosphorylation was enhanced only in GFP[+] fractions (supplemental Figure 1A). By using this MPN model, we evaluated the accumulation of DNA damage by immunofluorescence staining of γH2AX. We analyzed all the bone marrow cells 2 months after transplantation to exclude not only the stress of transplantation that may induce ROS and DNA damage effects but also the age-related changes. Lineage[−]c-Kit^{+} cells were isolated in each fraction for assessing DNA damage to decrease the influence of population differences between JAK2V617F[+] and JAK2V617F[−] bone marrow cells (supplemental Figure 1B-C). Surprisingly, both GFP[+] and GFP^{−} cells in MPN bone marrow showed similarly increased γH2AX foci formation compared with control GFP-reconstituted bone marrow cells, which rarely contained cells with γH2AX foci (Figure 1B-C). These results indicate that normal clones as well as JAK2V617F-harboring ones within MPN bone marrow have accumulated DNA damage.

JAK2V617F^{+} cells induce oxidative DNA damage in neighboring normal cells in a paracrine manner

Next, we were interested in whether the DNA damage response observed in GFP^{−} cells within MPN bone marrow is caused through the microenvironment of MPN bone marrow, or directly induced by JAK2V617F^{+} cells in a paracrine manner. To test these hypotheses

in vitro, murine myeloid cell line 32D cells were retrovirally transduced with JAK2V617F (JAK2V617F-32D), WT JAK2 (JAK2WT-32D), or GFP empty vector (EV-32D). Murine Mpl was also introduced into them as a homodimeric type I receptor, which is necessary for cytokine-independent JAK-STAT signaling activation mediated by JAK2V617F in 32D cells.[38] As previously described, the cells with coexpression of JAK2V617F and Mpl acquired constitutive activation of the JAK-STAT pathway (supplemental Figure 2A). To assess the paracrine effects induced by JAK2V617F clones, the parental 32D cells were cultured with the media conditioned by JAK2V617F-32D, JAK2WT-32D, or EV-32D and assessed for γH2AX foci formation (Figure 2A). As with the data we obtained in the murine MPN model, exposure of parental 32D cells to the CM derived from JAK2V617F-32D led to significant increase of γH2AX foci formation (Figure 2B and supplemental Figure 2B) and intracellular ROS levels (Figure 2C). Furthermore, the 32D cells cultured in JAK2V617F-CM showed decreased proliferation compared with the control (Figure 2D). When *N*-acetyl-*L*-cysteine was added into the JAK2V617F-CM, the phenotypes reverted to normal. Consistent with ROS accumulation, 32D cells treated with JAK2V617F-CM showed elevated levels of 8-hydroxy-2-deoxyguanosine (Figure 2E and supplemental Figure 2C). We further evaluated other types of DNA damage: immunoblotting of XPA for base or nucleotide excision repair against single-stranded DNA damage, and immunofluorescence staining for cyclobutane pyrimidine dimer formation, which did not show significant changes among samples (supplemental Figure 2D-E). Collectively, these results suggest that JAK2V617F[+] clones confer oxidative stress-induced DNA damage to coexisting normal cells via a paracrine mechanism independent of bone marrow microenvironment, and thereafter, the damaged normal hematopoietic cells activate a DNA damage response and suppress their proliferation.

Enhanced secretion of lipocalin-2 by JAK2V617F-harboring cells induces oxidative DNA damage in neighboring cells

Then, we conducted a search for the responsible factors associated with JAK2V617F-induced paracrine DNA damage. As a screening,
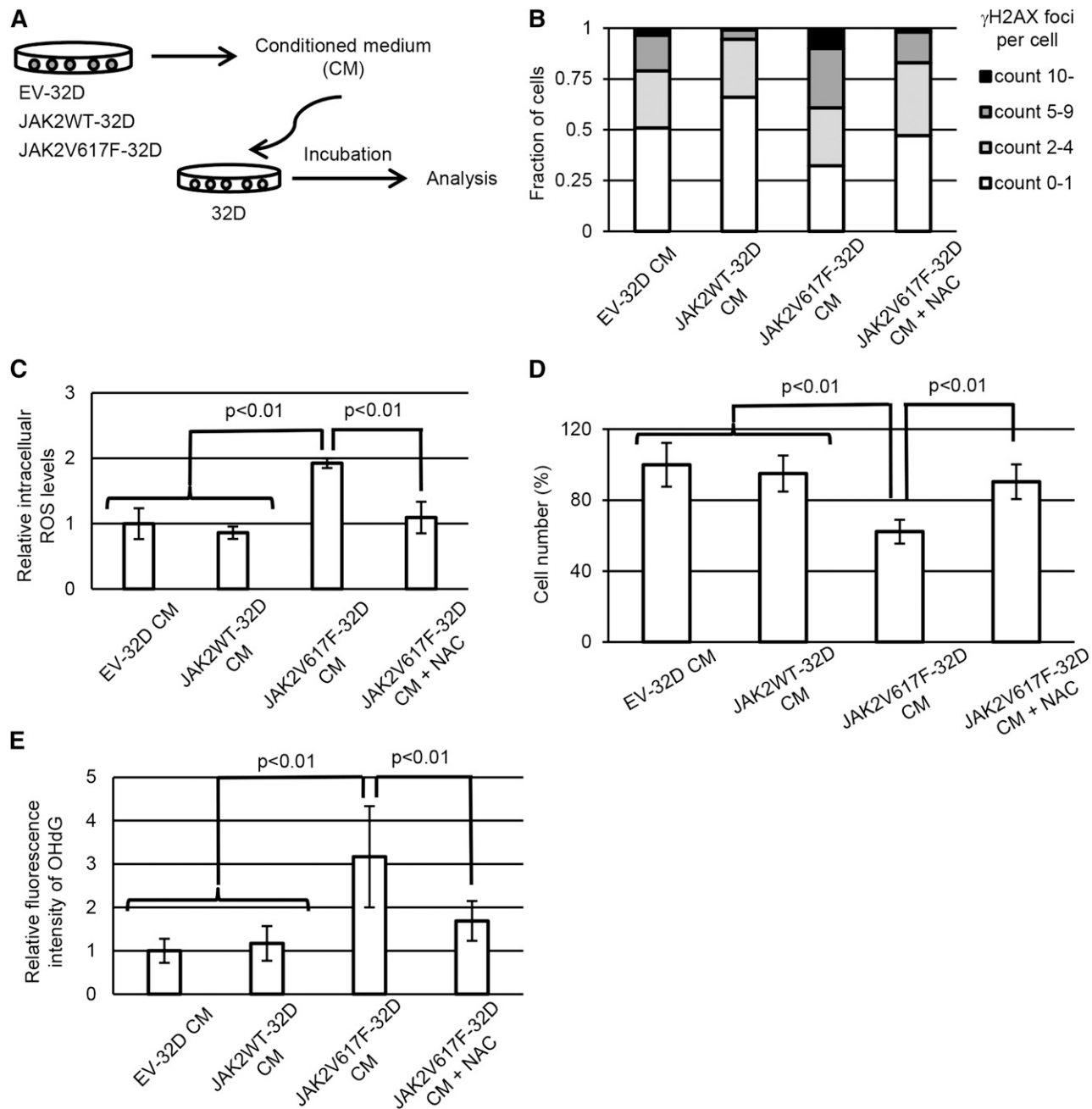
Figure 2. JAK2V617F^{+} hematopoietic cells induce DNA damage response in normal cells via paracrine signaling. (A) Schematic representation of the following experiments. EV-32D, JAK2WT-32D, and JAK2V617F-32D cells were cultured at a concentration of 1×10^6 cells per milliliter for 24 hours, and parental 32D cells were incubated at a concentration of 1×10^5 cells per milliliter with CM. (B) Immunofluorescence staining of γH2AX foci formation in parental 32D cells incubated with EV-32D CM, JAK2WT-32D CM, and JAK2V617F-32D CM with or without 1 mM of N-acetylcysteine (NAC). Distribution of the numbers of γH2AX foci per nucleus is shown. More than 100 cells were counted in each specimen. (C) Intracellular levels of ROS were measured by 2′,7′-dichlorodihydrofluorescein diacetate (H2DCFDA) assay following incubation of parental 32D cells with each CM with or without 1 mM NAC for 24 hours. Average mean fluorescein isothiocyanate (FITC) fluorescence intensity is shown (n = 3 each). (D) Relative cell numbers of parental 32D cells 36 hours after incubation with each CM with or without 1 mM NAC (n = 4 each). (E) Immunofluorescence staining of 8-hydroxy-2-deoxyguanosine (8-OHdG) in parental 32D cells incubated with EV-32D CM, JAK2WT-32D CM, and JAK2V617F-32D CM with or without 1 mM of NAC. Average fluorescence intensity of intranuclear 8-OHdG is shown. More than 100 cells were counted in each specimen. Error bars indicate standard deviation (SD).

we thoroughly investigated the genes with an increased expression in JAK2V617F^{+} hematopoietic cells compared with their normal counterparts through analysis of both murine and human gene expression profiles (GSE21842 and GSE9827; Figure 3A). In total, 21 genes were commonly upregulated in JAK2V617F^{+} cells, among which we focused on 8 genes encoding soluble factors as candidates for paracrine signaling associated with DNA damage. We confirmed by quantitative PCR that 6 of the 8 genes were indeed highly

expressed in JAK2V617F-32D cells compared with EV-32D cells (Figure 3B). For individually assessing the influence of these genes on paracrine DNA damage, we designed shRNA targeting each of them (supplemental Figure 3A), transduced it into JAK2V617F-32D cells, and tested the change in DNA damage response (Figure 3C and supplemental Figure 3B). First, for the purpose of screening candidate genes, we evaluated the growth-inhibiting effects of JAK2V617F-CM as a result of oxidative DNA damage. As shown in
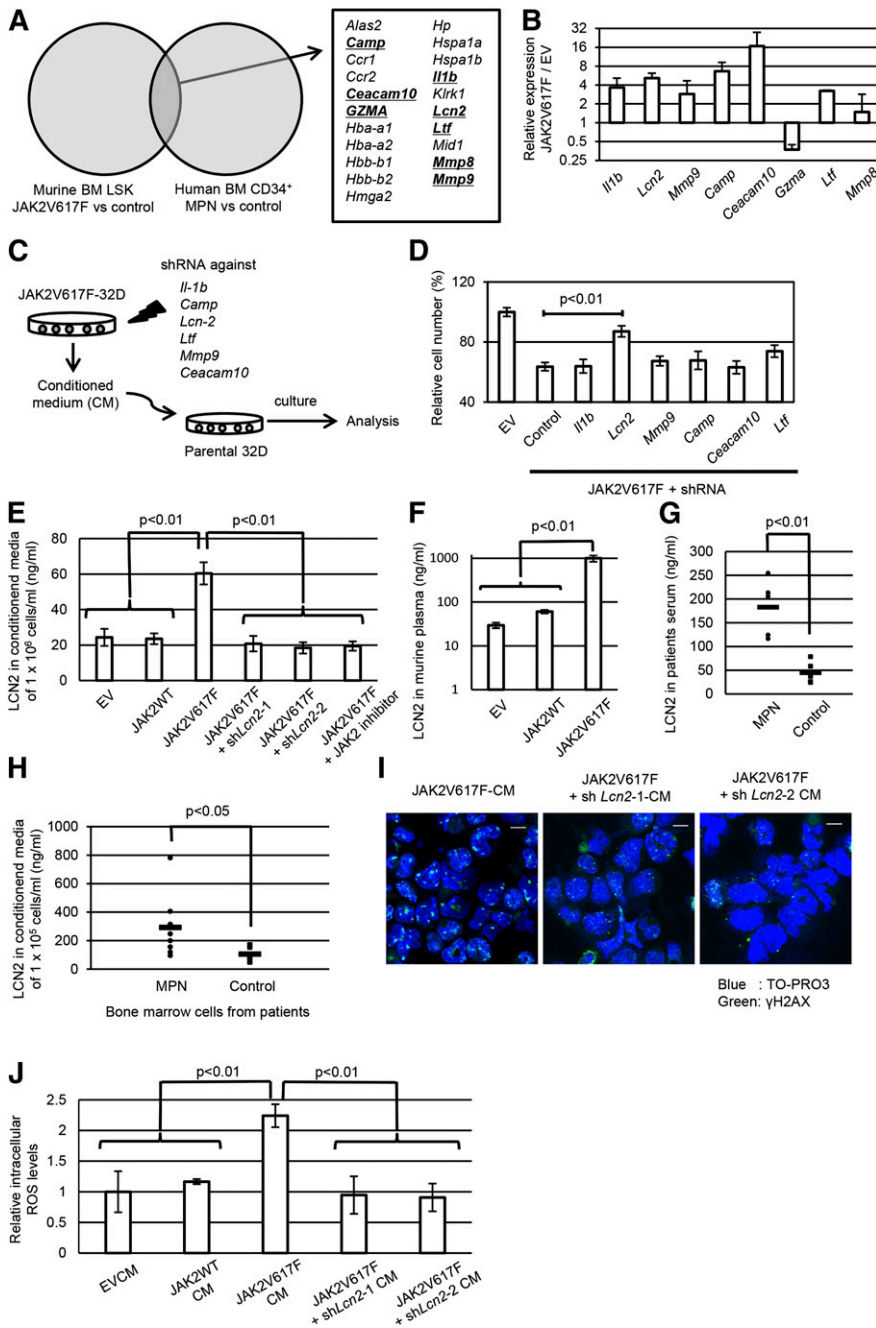
Figure 3. Lipocalin-2 secreted from JAK2V617F^{+} hematopoietic cells is associated with paracrine DNA damage. (A) Thorough investigation of genes with elevated expression in murine and human JAK2V617F^{+} hematopoietic cells compared with their normal counterparts in the published gene expression data (GSE21842 and GSE9827). Genes coding for soluble factors are underlined. (B) Quantitative real-time polymerase chain reaction (PCR) analysis of the candidate genes in JAK2V617F-32D cells relative to EV-32D cells (n = 3). (C) Schematic representation of the following experiments. JAK2V617F-32D cells were transduced with the shRNAs against candidate genes, and parental 32D cells were incubated with each CM. (D) Relative cell numbers of 32D cells 36 hours after incubation with each CM (n = 3 each). (E) Lipocalin-2 secretory ability in the respective 32D cells assessed by enzyme-linked immunosorbent assay (ELISA) in cultured media (n = 4 each). (F) Lipocalin-2 ELISA in the plasma of mice transplanted with EV, wild-type JAK2, or JAK2V61F-transduced bone marrow cells (n = 4 each). (G) Serum levels of lipocalin-2 in patients with MPNs. The concentration of lipocalin-2 for patients in complete remission for hematologic malignancies was measured as control. (H) Lipocalin-2 concentration of media conditioned by bone marrow mononuclear cells derived from patients with MPNs and controls. (I) Immunofluorescence staining of γH2AX foci formation (Alexa Fluor 488: green) in 32D cells incubated with CM from JAK2V617F-32D with shRNA against Lcn2 or control shRNA. Nuclei were stained with TO-PRO3. (J) Intracellular levels of ROS were measured by H2DCFDA assay following incubation of parental 32D cells with each CM for 24 hours. Average FITC fluorescence intensity is shown (n = 3 each). Scale bars: 10 μm. Error bars indicate SD.

Figure 3D, only when shRNA against *Lcn2* was transduced into JAK2V617F-32D cells was the growth-inhibiting effect of the JAK2V617F-CM clearly cancelled. Similar results were also observed in another shRNA targeting *Lcn2* (supplemental Figure 3C).

Before further exploring the influence of *Lcn2* knockdown on JAK2V617F^{+} cells, we confirmed that lipocalin-2 is significantly enriched in JAK2V617F-CM, and the knockdown of *Lcn2* or treatment with JAK2 inhibitor ruxolitinib reduced the concentration of lipocalin-2 in JAK2V617F-CM to almost the same level as that in EV-CM (Figure 3E). Previous studies have reported that the *Lcn2* promoter region contains a consensus binding site for STAT5.[37] We examined the transcriptional activity of this site in JAK2V617F-32D cells and found that the existence of this sequence, but not the mutated one, significantly enhanced the promoter activity, indicating that the expression of *Lcn2* is directly regulated by JAK-STAT

signaling (supplemental Figure 3D). Furthermore, plasma concentration of lipocalin-2 in JAK2V617F-induced MPN mice and the relative expression levels of *Lcn2* in JAK2V617F-transduced bone marrow cells were much higher compared with levels in the controls (Figure 3F and supplemental Figure 4A). The lipocalin-2 levels in MPN mice were significantly reduced by treatment with JAK2 inhibitor (supplemental Figure 4B). Next, we investigated the abundance of lipocalin-2 in patients with MPN. Although there was a considerable variation in serum levels of lipocalin-2 among the patients, the levels were significantly higher compared with those of controls (Figure 3G). In addition, MPN bone marrow cells secreted a significantly higher amount of lipocalin-2 than non-MPN control cells (Figure 3H and supplemental Table 3).

Then, we directly examined the effect of lipocalin-2 on DNA damage induction. Importantly, the enhanced levels of γH2AX
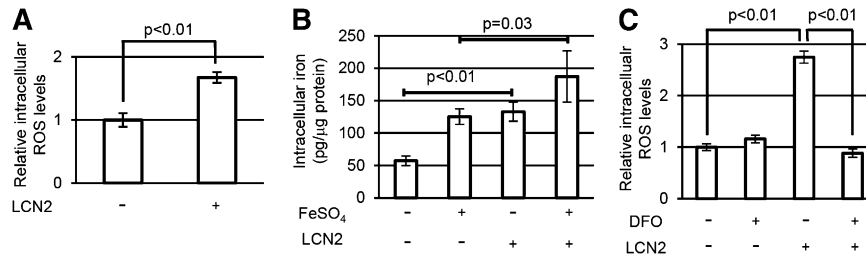
Figure 4. Lipocalin-2 induces oxidative DNA damage by elevating intracellular iron levels. (A) Intracellular levels of ROS in 32D cells were measured by H2DCFDA dye assay following their incubation with or without 100 ng/mL recombinant lipocalin-2 for 24 hours. Average mean FITC fluorescence intensity is shown (n = 3 each). (B) Intracellular iron levels of 32D cells with or without treatment with 100 ng/mL lipocalin-2 with or without 1 mM FeSO$_4$. The total cellular iron content was measured by the ferrozine method and normalized for protein content. (C) 32D cells were treated with 100 ng/mL lipocalin-2 and/or 2 μM deferoxamine (DFO). Intracellular ROS levels were measured by H2DCFDA dye assay 24 hours after incubation (n = 4 each). Error bars indicate SD.

foci formation evoked by JAK2V617F-CM were normalized when *Lcn2* was knocked down (Figure 3I). Moreover, intracellular ROS levels of parental 32D cells were also reduced when they were cultured in *Lcn2*-suppressed JAK2V617F-CM (Figure 3J). Collectively, these results indicate that lipocalin-2 abundantly secreted from JAK2V617F$^+$ clones should be associated with oxidative DNA damage induction into neighboring cells in a paracrine manner.

Lipocalin-2 induces oxidative DNA damage through intracellular iron overload

Next, we analyzed the mechanism of lipocalin-2 for triggering DNA damage response through intracellular ROS accumulation. We confirmed that exogenous treatment with recombinant lipocalin-2 led to significant elevation of intracellular ROS levels (Figure 4A). Because previous studies have reported that lipocalin-2 has a role of transporting iron inside the cells[39,40] and that excessive intracellular iron promotes oxidative stress,[41] we examined the relationship between lipocalin-2 treatment and intracellular iron uptake in hematopoietic cells. We quantified iron concentration within total cell lysates of 32D cells with or without treatment with lipocalin-2. Interestingly, 32D cells exposed to lipocalin-2 had significantly higher levels of intracellular iron, and the effect was further enhanced with addition of FeSO$_4$ to the medium (Figure 4B). Consistent with the results, intracellular ROS levels enhanced by lipocalin-2 reverted to normal with cotreatment of iron-chelating agent deferoxamine (Figure 4C). These results indicate that the paracrine oxidative stress effects of lipocalin-2 are mediated by intracellular iron overload, and iron chelating agents are effective for normalizing the effect.

Lipocalin-2–induced DNA damage response is associated with p53 pathway activation

We further studied the response of normal hematopoietic cells to lipocalin-2–induced DNA damage. Treatment of 32D cells with JAK2V617F-32D CM significantly increased the rate of apoptosis (Figure 5A), which is consistent with decreased cellular proliferation by the CM (Figure 2E). Moreover, the expression levels of proapoptotic genes such as *Bax*, *Pmaip1*, and *Bbc3* were elevated in the JAK2V617F-CM–treated 32D cells (Figure 5B). Since these genes are regulated by p53, we analyzed its pathway activity and found that both total and phosphorylated p53 were elevated in JAK2V617F-CM–treated 32D cells (Figure 5C), suggesting that p53 pathway has been activated in the cells accompanied by DNA damage, which led to increased apoptosis of the severely damaged cells. Similarly, 32D cells and murine bone marrow cells showed increased levels of p53 and elevated apoptosis in response to lipocalin-2 (Figure 5D-F). In contrast, lipocalin-2 had no effect on

proliferation against the p53-deficient cells (Figure 5G). These results demonstrate that lipocalin-2 induces p53 pathway activation against DNA damage in normal hematopoietic cells, which results in increased apoptosis and reduced cellular proliferation.

Lipocalin-2 induces growth advantage of JAK2V617F$^+$ cells over normal hematopoietic cells

We further investigated the autocrine effects of lipocalin-2 on JAK2V617F$^+$ cells themselves. First, we confirmed that both JAK2V617F-32D and EV-32D cells showed a similar increase in intracellular ROS levels upon treatment with lipocalin-2 (Figure 6A). In contrast with EV-32D cells, however, 32D-JAK2V617F cells escaped growth suppression when exposed to lipocalin-2 (Figure 6B). Moreover, JAK2V617F-32D cells showed no significant increase in apoptosis when incubated with lipocalin-2–enriched medium (Figure 6C), which contrasted with the data for control 32D cells (Figure 5A). To exclude the influence of autonomous lipocalin-2 secretion, we used bone marrow cells derived from lipocalin-2–deficient mice. When bone marrow c-Kit$^+$ cells transduced with JAK2V617F or EV were evaluated for their colony-forming capacity, lipocalin-2 reduced colony-forming capacity in EV-transduced cells, but not in JAK2V617F$^+$ cells (Figure 6D). We also confirmed that normal bone marrow cells showed decreased cell proliferation when cocultured with JAK2V617F-transduced *Lcn2*$^{+/+}$ bone marrow cells, whereas they proliferated normally when cocultured with JAK2V617F-transduced *Lcn2*$^{-/-}$ bone marrow cells (Figure 6E). JAK2V617F$^+$ cells did not show increase in p53 when treated with lipocalin-2, which presented a sharp contrast with normal bone marrow cells (Figure 6F). Lipocalin-2 also reduced colony-forming capacity for human non-MPN bone marrow cells, but not for MPN cells (Figure 6G).

We were then interested in how JAK2V617F$^+$ cells escaped from the growth-inhibitory effects of lipocalin-2. On the basis of a previous study showing that JAK2V617F$^+$ cells have elevated levels of MDM2, which destabilizes p53 and prevents its upregulation upon DNA damage,[42] we speculated that MDM2 is the key mediator that induces differences in proliferation. To investigate this hypothesis, we first confirmed that JAK2V617F-32D cells had increased protein level of MDM2 (Figure 6H). Moreover, when cotreated with the MDM2 inhibitor nutlin-3, lipocalin-2 also suppressed the proliferation of JAK2V617F-32D cells (Figure 6I), indicating that JAK2V617F$^+$ cells have a reduced response to DNA damage as a result of elevated MDM2, which confers relative growth advantage to themselves through secretion of lipocalin-2.

Finally, we evaluated the impact of lipocalin-2 oversecretion on the propagation of JAK2V617F$^+$ cells in vivo. Bone marrow c-Kit$^+$ cells transduced with JAK2V617F followed by shRNA against
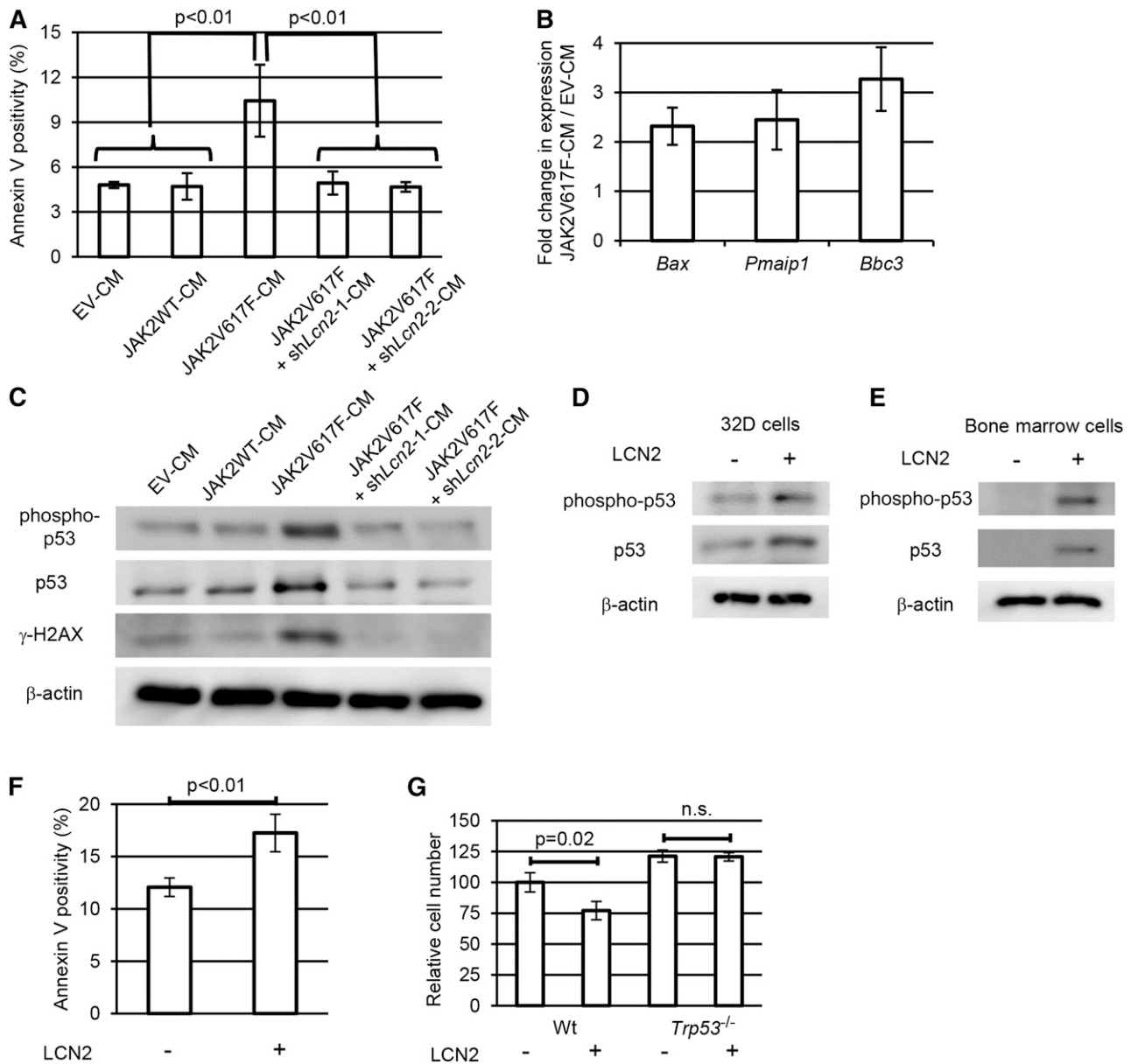
Figure 5. Lipocalin-2 suppresses normal hematopoietic cell growth through activation of the p53 pathway. (A) Average percent increase of apoptosis in parental 32D cells treated with each CM (n = 3 each). (B) Quantitative real-time PCR analysis of a subset p53 target genes in 32D cells treated with 32D-JAK2V617F CM relative to those with EV-32D CM (n = 3). (C) Immunoblotting of p53 and phospho-p53 in 32D cells incubated with CM of EV-32D, JAK2WT-32D, or JAK2V617F-32D with or without shRNA against *Lcn2*. (D-E) Immunoblotting of p53 and phospho-p53 in (D) 32D cells and (E) murine bone marrow c-Kit$^+$ cells with or without exposure to 100 ng/mL lipocalin-2. (F) Average percent increase of apoptosis in murine bone marrow c-Kit$^+$ cells when treated with 100 ng/mL lipocalin-2. (G) Relative cell numbers of wild-type or *Trp53*-deficient murine bone marrow c-Kit$^+$ cells after 36 hours incubation with or without 100 ng/mL lipocalin-2 (n = 3 each). Error bars indicate SD. n.s., not significant.

Lcn2 were transplanted into sublethally irradiated mice (Figure 7A). Although JAK2V617F$^+$ cells with knockdown of *Lcn2* were still able to repopulate in the recipient bone marrow, they showed significantly reduced engraftment compared with the control (Figure 7B). Collectively, these results show that lipocalin-2 secreted from JAK2V617F$^+$ MPN clones confers a relative growth advantage to themselves via suppression of normal hematopoietic cells.

Discussion

During out research, we studied pathogenesis underlying the increased risk for leukemogenesis in patients with MPNs. Of note,

we shed light on the enigmatic phenomena that leukemic clones develop from JAK2V617F$^-$ clones as well as from the mutation-positive clones. Surprisingly, in the murine MPN model, we found that JAK2V617F$^-$ normal clones accumulated DNA damage as much as did the JAK2V617F$^+$ MPN clones. Comprehensive screening of the genes identified that soluble-factor lipocalin-2 had an important role for inducing oxidative DNA damage. These results are consistent with the clinical findings that both MPN clones and neighboring JAK2V617F$^-$ clones have risks for transforming to leukemia through acquired mutations. In addition, lipocalin-2 suppressed normal hematopoietic cells, but not JAK2V617F$^+$ ones, which contributed to a relative growth advantage for MPN clones (Figure 7C).

A mechanism for explaining the evolution of JAK2V617F$^-$ AML clones from JAK2V617F$^+$ MPNs has recently been actively

Figure 6. JAK2V617F$^+$ cells escape from lipocalin-2–induced growth suppression resulting from attenuated p53 activation. (A) Intracellular levels of ROS in 32D cells transduced with Kusabira-Orange empty vector or JAK2V617F-IRES-Kusabira-Orange were measured by H2DCFDA dye assay following exposure to 100 ng/mL recombinant lipocalin-2 for 24 hours. Average mean FITC fluorescence intensity is shown (n = 4 each). (B) Relative numbers of 32D cells with empty vector or JAK2V617F after 36 hours incubation with or without 100 ng/mL lipocalin-2 (n = 4 each). (C) Average apoptotic cell ratio in JAK2V617F-32D cells treated with each CM (n = 4 each). (D) Colony-forming cell assay for *Lcn2*-deficient murine bone marrow c-Kit$^+$ cells transduced with empty vector or JAK2V617F with or without 100 ng/mL lipocalin-2 (n = 4 each). (E) Relative cell numbers of normal bone marrow c-Kit$^+$ cells 48 hours after incubation with wild-type or *Lcn2*$^{-/-}$ bone marrow cells transduced with JAK2V617F-IRES-GFP (n = 4 each). In coculture experiments, the number of normal bone marrow cells was counted by multiplying the total number of cells by the fraction of GFP$^-$ cells. (F) Immunoblotting of p53 and phospho-p53 in *Lcn2*-deficient murine bone marrow c-Kit$^+$ cells transduced with empty vector or JAK2V617F with or without 100 ng/mL lipocalin-2. (G) Colony-forming cell assay for bone marrow CD34$^+$ cells from patients with MPN and non-MPN control patients with or without 1 μg/mL recombinant lipocalin-2. Cells were seeded in semisolid medium (Methocult H4434 Classic; StemCell Technologies). The total numbers of colonies per 1000 cells are shown. The colony numbers were compared between wells with or without lipocalin-2 by using paired Student *t* tests. Detailed patient characteristics are described in supplemental Table 3. (H) Immunoblotting of MDM2 in 32D cells with empty vector or JAK2V617F. (I) Relative cell numbers of 32D cells with empty vector or JAK2V617F after 36 hours incubation with or without 100 ng/mL lipocalin-2 and 0.5 μM nutlin-3 (n = 4 each). Error bars indicate SD.
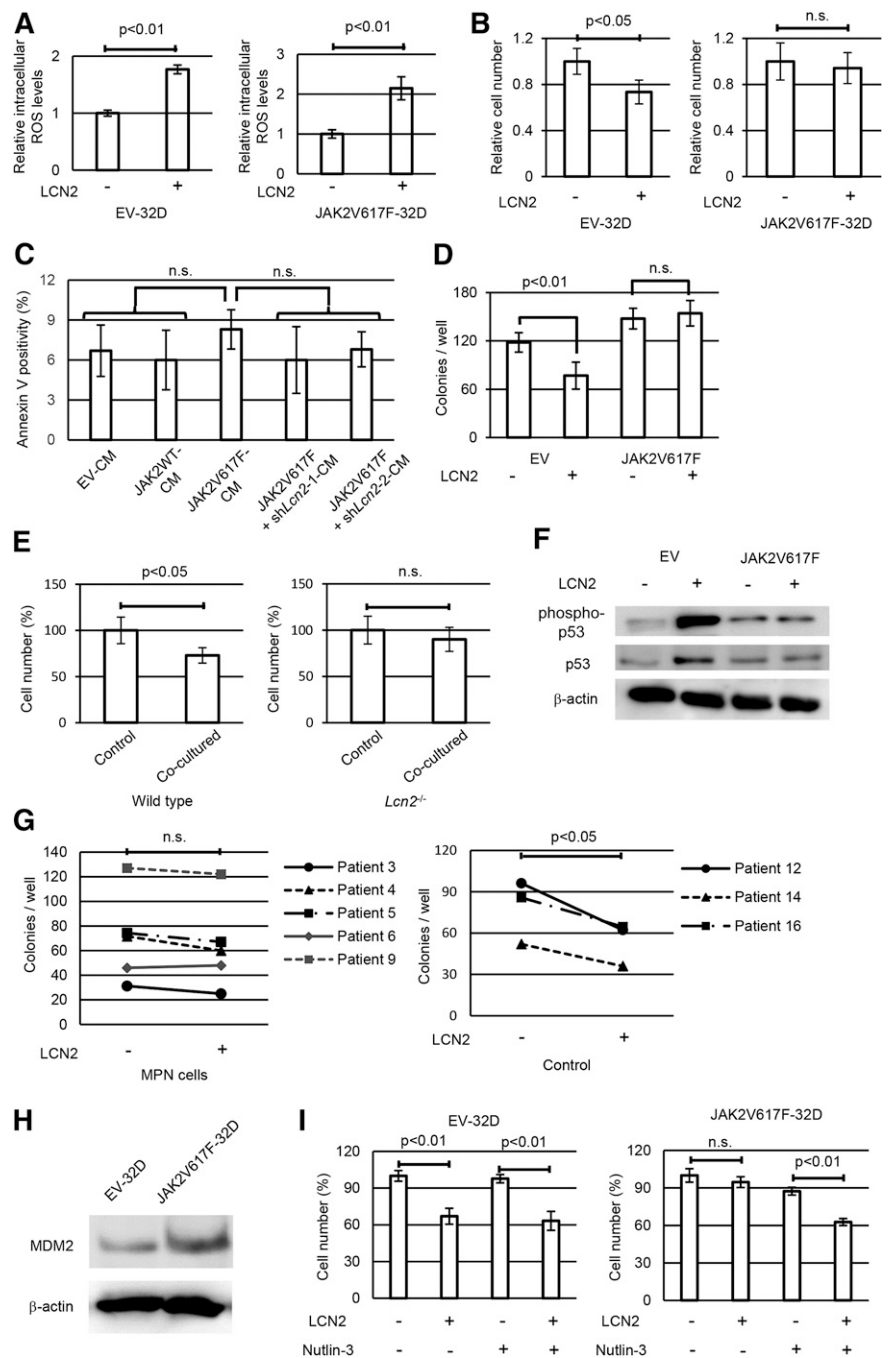
discussed.[29,30] Although there was a report showing that *TET2* mutation was precedent to *JAK2* mutation, the *TET2* mutation can also occur as a late event in other cases, suggesting that the order of mutation acquisition is not essential.[43,44] In any case, further accumulation of genetic events after the MPN phase is required for leukemic transformation, and there should exist a mechanism for propelling the events in MPN. Our study suggests that lipocalin-2 could take a role as one of the accelerators in leukemogenesis through induction of DNA damage. Our finding is unique in that lipocalin-2 acts on neighboring normal cells in paracrine fashion. As for the mechanism of lipocalin-2–induced oxidative stress, we showed that it increased intracellular iron uptake, which led to intracellular ROS elevation. Iron overload is a major cause of oxidative stress in

myelodysplastic syndrome patients, primarily as a result of regular transfusions.[45] Our results could provide promising strategies for reducing the risk for leukemic transformation from MPNs. There has also been some evidence that lipocalin-2 is associated with the induction of other proinflammatory cytokines such as tumor necrosis factor α and IL-1β, which might also be related to the DNA damage through enhancing intra–bone marrow inflammatory states.[46,47] Further studies are required for elucidating an effect of lipocalin-2 in vivo. In addition to JAK2V617F, we showed that JAK2V617F$^-$ MPN cells with insertion mutations in calreticulin (CALR) also had increased secretory capacities for lipocalin-2, which is reasonable considering that those mutations induce constitutive activation of the JAK-STAT pathway.[48]
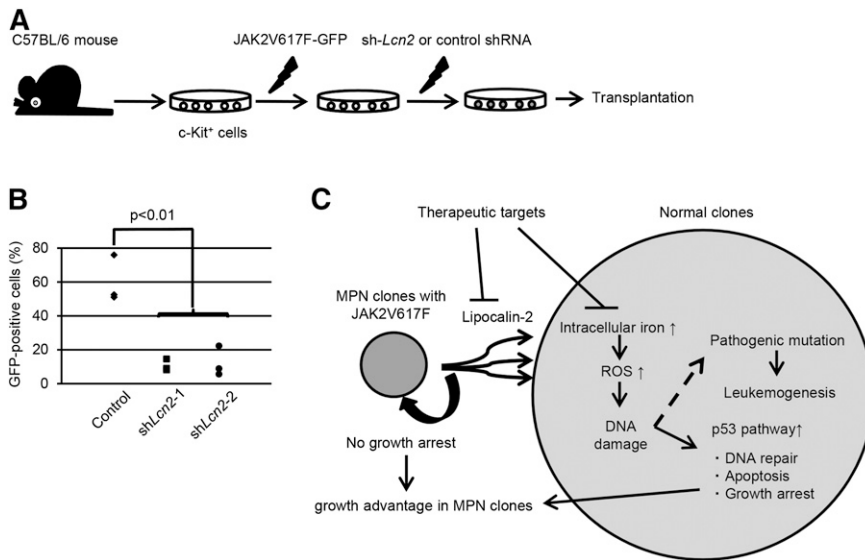
Figure 7. Lipocalin-2 abundantly secreted from JAK2V617F$^+$ cells confers growth advantage to MPN cells. (A) Schematic representation of the following experiments. Murine bone marrow c-Kit$^+$ cells were retrovirally transduced with JAK2V617F followed by shRNA against *Lcn2* or control shRNA and transplanted into sublethally irradiated mice. (B) Repopulated GFP$^+$ cells within bone marrow mononuclear cells were analyzed 6 weeks after transplantation. Three mice were analyzed for each shRNA. (C) Proposed mechanisms whereby JAK2V617F$^+$ clones induce paracrine DNA damage and acquire clonal dominance via secretion of lipocalin-2.

Conversely, although patients with MPN have an increased risk for leukemic transformation compared with the general population, cumulative incidence rate is still low during long-term follow-up. As indicated in our study, normal hematopoietic cells have a safeguarding mechanism against DNA damage in which the p53 pathway plays an essential role for preventing the emergence of aberrant clones. Indeed, *TP53* mutation is seen in about 20% of the patients with post-MPN AML and is one of the most common mutations among them,[25,30,49] whereas the mutation is reported in approximately 10% of de novo AML patients, indicating an especially crucial role of the pathway in preventing leukemogenesis from MPNs.[50] Alternatively, increased DNA damage responses could result in an error in DNA repair and acquisition of aberrant mutations. Although there is some evidence that quiescent hematopoietic stem cells more often use error-prone nonhomologous end joining rather than homologous recombination for repairing DNA double-strand breaks,[51] they are considered to be vulnerable to acquiring mutations for DNA damage.

Another equally important aspect of lipocalin-2 secretion from JAK2V617F$^+$ cells is that it inhibits the growth of normal hematopoietic cells. Although lipocalin-2–mediated suppression of normal hematopoiesis has been reported in the BCR-ABL–induced murine chronic myeloid leukemia model, its precise mechanism remains to be elucidated.[52,53] We hypothesized that the growth suppression resulted from the p53 pathway activation after DNA damage. Consistent with the concept, lipocalin-2 did not suppress proliferation of p53-deficient bone marrow cells. Interestingly, JAK2V617F$^+$ cells did not suffer from growth suppression by lipocalin-2 as in BCR-ABL$^+$ cells, which led to the relative growth advantage of the clones. These data explain how JAK2V617F$^+$ cells accomplish clonal expansion despite their impaired hematopoietic stem cell function.[16,54] Therefore, blocking lipocalin-2 secretion is considered beneficial for preventing propagation of MPN clones.

Collectively, lipocalin-2 secreted from MPN clones leads to initiation of malignant clones through DNA damage accumulation and supports their proliferation via suppression of the surrounding clones. There have been several studies showing that JAK-STAT signaling pathway is upregulated in different types of cancers.[55,56] Inhibition of the signaling cascade might contribute to the alleviation of genetic instability induced by the tumor microenvironment.

Acknowledgments

Authorship

Contribution: Y.K. designed research, performed experiments, analyzed data, and wrote the manuscript; A.Y. and T.T.-K. performed experiments on a murine JAK2V617F MPN model and performed the analysis for DNA damage; S. Arai designed research and analyzed data; T.S. and S. Akira helped perform experiments using *Lcn2*-knockout mice; and M.K. designed the research and supervised the entire project.

Conflict-of-interest disclosure: The authors declare no competing financial interests.

Correspondence: Mineo Kurokawa, Department of Hematology and Oncology, Graduate School of Medicine, The University of Tokyo, 7-3-1 Hongo, Bunkyo-ku, Tokyo 113-8655, Japan; e-mail: kurokawa-tky@umin.ac.jp.

References

1. Baxter EJ, Scott LM, Campbell PJ, et al; Cancer Genome Project. Acquired mutation of the tyrosine kinase JAK2 in human myeloproliferative disorders. *Lancet.* 2005;365(9464):1054-1061.

2. James C, Ugo V, Le Couédic JP, et al. A unique clonal JAK2 mutation leading to constitutive signalling causes polycythaemia vera. *Nature.* 2005;434(7037):1144-1148.

3. Jones AV, Kreil S, Zoi K, et al. Widespread occurrence of the JAK2 V617F mutation in chronic myeloproliferative disorders. *Blood.* 2005;106(6):2162-2168.

4. Kralovics R, Passamonti F, Buser AS, et al. A gain-of-function mutation of JAK2 in myeloproliferative disorders. *N Engl J Med.* 2005;352(17):1779-1790.

5. Levine RL, Wadleigh M, Cools J, et al. Activating mutation in the tyrosine kinase JAK2 in polycythemia vera, essential thrombocythemia, and myeloid metaplasia with myelofibrosis. *Cancer Cell.* 2005;7(4):387-397.

6. Najean Y, Rain JD. The very long-term evolution of polycythemia vera: an analysis of 318 patients initially treated by phlebotomy or 32P between 1969 and 1981. *Semin Hematol.* 1997;34(1):6-16.

7. Abdel-Wahab O, Manshouri T, Patel J, et al. Genetic analysis of transforming events that convert chronic myeloproliferative neoplasms to leukemias. *Cancer Res.* 2010;70(2):447-452.

8. Wolanskyj AP, Schwager SM, McClure RF, Larson DR, Tefferi A. Essential thrombocythemia beyond the first decade: life expectancy, long-term complication rates, and prognostic factors. *Mayo Clin Proc.* 2006;81(2):159-166.

9. Gaidano G, Guerrasio A, Serra A, Rege-Cambrin G, Saglio G. Molecular mechanisms of tumor progression in chronic myeloproliferative disorders. *Leukemia.* 1994;8(Suppl 1):S27-S29.

10. Mesa RA, Li CY, Ketterling RP, Schroeder GS, Knudson RA, Tefferi A. Leukemic transformation in myelofibrosis with myeloid metaplasia: a single-institution experience with 91 cases. *Blood.* 2005;105(3):973-977.

11. Bumm TG, Elsea C, Corbin AS, et al. Characterization of murine JAK2V617F-positive myeloproliferative disease. *Cancer Res.* 2006;66(23):11156-11165.

12. Lacout C, Pisani DF, Tulliez M, Gachelin FM, Vainchenker W, Villeval JL. JAK2V617F expression in murine hematopoietic cells leads to MPD mimicking human PV with secondary myelofibrosis. *Blood.* 2006;108(5):1652-1660.

13. Wernig G, Mercher T, Okabe R, Levine RL, Lee BH, Gilliland DG. Expression of Jak2V617F causes a polycythemia vera-like disease with associated myelofibrosis in a murine bone marrow transplant model. *Blood.* 2006;107(11):4274-4281.

14. Shide K, Shimoda HK, Kumano T, et al. Development of ET, primary myelofibrosis and PV in mice expressing JAK2 V617F. *Leukemia.* 2008;22(1):87-95.

15. Xing S, Wanting TH, Zhao W, et al. Transgenic expression of JAK2V617F causes myeloproliferative disorders in mice. *Blood.* 2008;111(10):5109-5117.

16. Mullally A, Lane SW, Ball B, et al. Physiological Jak2V617F expression causes a lethal myeloproliferative neoplasm with differential effects on hematopoietic stem and progenitor cells. *Cancer Cell.* 2010;17(6):584-596.

17. Marty C, Lacout C, Martin A, et al. Myeloproliferative neoplasm induced by constitutive expression of JAK2V617F in knock-in mice. *Blood.* 2010;116(5):783-787.

18. Akada H, Yan D, Zou H, Fiering S, Hutchison RE, Mohi MG. Conditional expression of heterozygous or homozygous Jak2V617F from its endogenous promoter induces a polycythemia vera-like disease. *Blood.* 2010;115(17):3589-3597.

19. Lundberg P, Karow A, Nienhold R, et al. Clonal evolution and clinical correlates of somatic mutations in myeloproliferative neoplasms. *Blood.* 2014;123(14):2220-2228.

20. Klampfl T, Harutyunyan A, Berg T, et al. Genome integrity of myeloproliferative neoplasms in chronic phase and during disease progression. *Blood.* 2011;118(1):167-176.

21. Abdel-Wahab O, Pardanani A, Rampal R, Lasho TL, Levine RL, Tefferi A. DNMT3A mutational analysis in primary myelofibrosis, chronic myelomonocytic leukemia and advanced phases of myeloproliferative neoplasms. *Leukemia.* 2011;25(7):1219-1220.

22. Ding Y, Harada Y, Imagawa J, Kimura A, Harada H. AML1/RUNX1 point mutation possibly promotes leukemic transformation in myeloproliferative neoplasms. *Blood.* 2009;114(25):5201-5205.

23. Taketani T, Taki T, Takita J, et al. Mutation of the AML1/RUNX1 gene in a transient myeloproliferative disorder patient with Down syndrome. *Leukemia.* 2002;16(9):1866-1867.

24. Pardanani A, Lasho TL, Finke CM, Mai M, McClure RF, Tefferi A. IDH1 and IDH2 mutation analysis in chronic- and blast-phase myeloproliferative neoplasms. *Leukemia.* 2010;24(6):1146-1151.

25. Harutyunyan A, Klampfl T, Cazzola M, Kralovics R. p53 lesions in leukemic transformation. *N Engl J Med.* 2011;364(5):488-490.

26. Sterkers Y, Preudhomme C, Laï JL, et al. Acute myeloid leukemia and myelodysplastic syndromes following essential thrombocythemia treated with hydroxyurea: high proportion of cases with 17p deletion. *Blood.* 1998;91(2):616-622.

27. Burkitt MJ, Raafat A. Nitric oxide generation from hydroxyurea: significance and implications for leukemogenesis in the management of myeloproliferative disorders. *Blood.* 2006;107(6):2219-2222.

28. Campbell PJ, Baxter EJ, Beer PA, et al. Mutation of JAK2 in the myeloproliferative disorders: timing, clonality studies, cytogenetic associations, and role in leukemic transformation. *Blood.* 2006;108(10):3548-3555.

29. Theocharides A, Boissinot M, Girodon F, et al. Leukemic blasts in transformed JAK2-V617F-positive myeloproliferative disorders are frequently negative for the JAK2-V617F mutation. *Blood.* 2007;110(1):375-379.

30. Beer PA, Delhommeau F, LeCouédic JP, et al. Two routes to leukemic transformation after a JAK2 mutation-positive myeloproliferative neoplasm. *Blood.* 2010;115(14):2891-2900.

31. Plo I, Nakatake M, Malivert L, et al. JAK2 stimulates homologous recombination and genetic instability: potential implication in the heterogeneity of myeloproliferative disorders. *Blood.* 2008;112(4):1402-1412.

32. Tsukada T, Tomooka Y, Takai S, et al. Enhanced proliferative potential in culture of cells from p53-deficient mice. *Oncogene.* 1993;8(12):3313-3322.

33. Flo TH, Smith KD, Sato S, et al. Lipocalin 2 mediates an innate immune response to bacterial infection by sequestering iron. *Nature.* 2004;432(7019):917-921.

34. Bersenev A, Wu C, Balcerek J, Tong W. Lnk controls mouse hematopoietic stem cell self-renewal and quiescence through direct interactions with JAK2. *J Clin Invest.* 2008;118(8):2832-2844.

35. Kagoya Y, Yoshimi A, Kataoka K, et al. Positive feedback between NF-κB and TNF-α promotes leukemia-initiating cell capacity. *J Clin Invest.* 2014;124(2):528-542.

36. Schmittgen TD, Livak KJ. Analyzing real-time PCR data by the comparative C(T) method. *Nat Protoc.* 2008;3(6):1101-1108.

37. Sheng Z, Wang SZ, Green MR. Transcription and signalling pathways involved in BCR-ABL-mediated misregulation of 24p3 and 24p3R. *EMBO J.* 2009;28(7):866-876.

38. Lu X, Levine R, Tong W, et al. Expression of a homodimeric type I cytokine receptor is required for JAK2V617F-mediated transformation. *Proc Natl Acad Sci USA.* 2005;102(52):18962-18967.

39. Devireddy LR, Gazin C, Zhu X, Green MR. A cell-surface receptor for lipocalin 24p3 selectively mediates apoptosis and iron uptake. *Cell.* 2005;123(7):1293-1305.

40. Iannetti A, Pacifico F, Acquaviva R, et al. The neutrophil gelatinase-associated lipocalin (NGAL), a NF-kappaB-regulated gene, is a survival factor for thyroid neoplastic cells. *Proc Natl Acad Sci USA.* 2008;105(37):14058-14063.

41. McCord JM. Iron, free radicals, and oxidative injury. *J Nutr.* 2004;134(11):3171S-3172S.

42. Nakatake M, Monte-Mor B, Debili N, et al. JAK2 (V617F) negatively regulates p53 stabilization by enhancing MDM2 via La expression in myeloproliferative neoplasms. *Oncogene.* 2012;31(10):1323-1333.

43. Couronné L, Lippert E, Andrieux J, et al. Analyses of TET2 mutations in post-myeloproliferative neoplasm acute myeloid leukemias. *Leukemia.* 2010;24(1):201-203.

44. Schaub FX, Looser R, Li S, et al. Clonal analysis of TET2 and JAK2 mutations suggests that TET2 can be a late event in the progression of myeloproliferative neoplasms. *Blood.* 2010;115(10):2003-2007.

45. Ghoti H, Fibach E, Merkel D, Perez-Avraham G, Grisariu S, Rachmilewitz EA. Changes in parameters of oxidative stress and free iron biomarkers during treatment with deferasirox in iron-overloaded patients with myelodysplastic syndromes. *Haematologica.* 2010;95(8):1433-1434.

46. Law IK, Xu A, Lam KS, et al. Lipocalin-2 deficiency attenuates insulin resistance associated with aging and obesity. *Diabetes.* 2010;59(4):872-882.

47. Jang E, Kim JH, Lee S, et al. Phenotypic polarization of activated astrocytes: the critical role of lipocalin-2 in the classical inflammatory activation of astrocytes. *J Immunol.* 2013;191(10):5204-5219.

48. Klampfl T, Gisslinger H, Harutyunyan AS, et al. Somatic mutations of calreticulin in myeloproliferative neoplasms. *N Engl J Med.* 2013;369(25):2379-2390.

49. Beer PA, Ortmann CA, Campbell PJ, Green AR. Independently acquired biallelic JAK2 mutations are present in a minority of patients with essential thrombocythemia. *Blood.* 2010;116(6):1013-1014.

50. Haferlach C, Dicker F, Herholz H, Schnittger S, Kern W, Haferlach T. Mutations of the TP53 gene in acute myeloid leukemia are strongly associated with a complex aberrant karyotype. *Leukemia.* 2008;22(8):1539-1541.

51. Mohrin M, Bourke E, Alexander D, et al. Hematopoietic stem cell quiescence promotes error-prone DNA repair and mutagenesis. *Cell Stem Cell.* 2010;7(2):174-185.

52. Lin H, Monaco G, Sun T, et al. Bcr-Abl-mediated suppression of normal hematopoiesis in leukemia. *Oncogene.* 2005;24(20):3246-3256.

53. Leng X, Lin H, Ding T, et al. Lipocalin 2 is required for BCR-ABL-induced tumorigenesis. *Oncogene.* 2008;27(47):6110-6119.

54. Li J, Spensberger D, Ahn JS, et al. JAK2 V617F impairs hematopoietic stem cell function in a conditional knock-in mouse model of JAK2 V617F-positive essential thrombocythemia. *Blood.* 2010;116(9):1528-1538.

55. Lee HJ, Daver N, Kantarjian HM, Verstovsek S, Ravandi F. The role of JAK pathway dysregulation in the pathogenesis and treatment of acute myeloid leukemia. *Clin Cancer Res.* 2013;19(2):327-335.

56. Vainchenker W, Constantinescu SN. JAK/STAT signaling in hematological malignancies. *Oncogene.* 2013;32(21):2601-2613.